Catalysis Science & Technology

Accepted Manuscript

ROYAL SOCIETY OF CHEMISTRY

www.rsc.org/catalysis

Journal Name

RSCPublishing

ARTICLE

Rhodium Diphosphine Complexes: a Case Study for Catalyst Activation and Deactivation

Cite this: DOI: 10.1039/xoxxoooooox

Antje Meißner,[a] Elisabetta Alberico,[b]* Hans-Joachim Drexler,[a] Wolfgang Baumann[a] and Detlef Heller[a]*

Received ooth January 2012,
Accepted ooth January 2012

DOI: 10.1039/xoxxoooooox

www.rsc.org/

The present work provides an overview of possible activation and deactivation phenomena in homogeneous catalytic processes promoted by different types of *rhodium complexes* containing *diphosphine ligands*. While awaiting for more efficient 1st row metal based catalysts, a more economic and greener approach to the use of expensive catalysts based on precious metals requires an in-depth knowledge of both the reaction mechanism *and* the activation and deactivation phenomena which may reduce the temporary solution concentration of the metal effectively available for catalysis. The present work provides in particular a quantitative description of activation and deactivation phenomena such as generation of active species from suitable precatalysts (induction periods); catalyst deactivation due to formation of non-reactive, monomeric species with either the solvent, the substrate, the product or additives; catalyst aggregation to usually non-reactive multinuclear complexes. Some critical remarks concerning the often applied 'in situ' procedure for 'catalyst' generation are also included.

1. Introduction

The term sustainability in chemistry is generally applied in reference to the atom-economic, efficient and environmentally friendly use of raw materials.[1] In other words, sustainable chemistry for which catalysis is a key technology, has been almost exclusively referred to the judicious choice of reagents and solvents, while neglecting the equally important sensible use of, often expensive, catalysts.

A catalyzed process is by definition '*greener*' than the uncatalyzed one because, by binding of the catalytic active complex to the substrate, a new reaction pathway opens up which unfolds under milder reaction conditions. Quite often, the catalyzed reaction is also more atom-economic and less polluting, avoiding the formation of stoichiometric amounts of by-products. In the last years further steps towards the implementation of more economically and environmentally friendly processes have been taken in the design of catalysts by replacing precious metals with more abundant and often less toxic ones.[2] However, catalysts based on first-row and main group elements have so far failed to provide the high efficiency required for immediate application. Therefore, while awaiting for improvements, a sensible and greener approach to the use of expensive catalysts would require an in-depth knowledge of the activation and deactivation phenomena which may reduce the temporary solution concentration of the metal effectively available for catalysis.

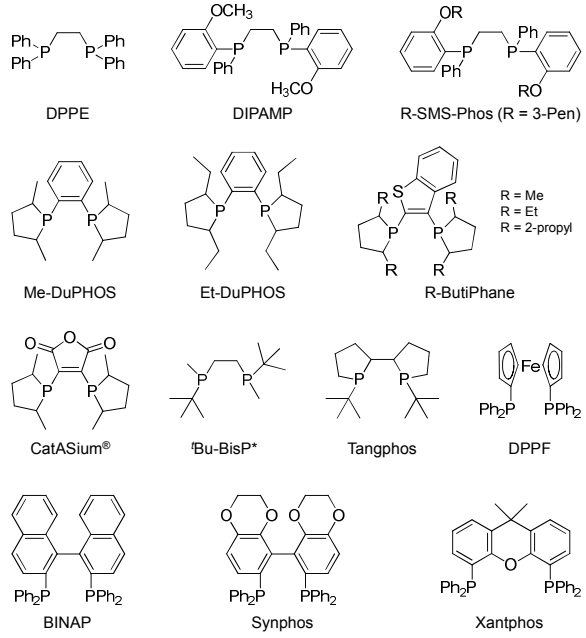

Figure 1 Structures of the diphosphine ligands which are discussed in this work.

Several events may affect the catalyst activity. The catalyst may undergo a modification which completely suppresses its activity: the irreversible thermal denaturation of enzymes is an example. The concentration of the catalytic active species, while being generated from a suitable catalyst precursor, can

vary over time being reflected in a macroscopic increase of catalyst activity. The reversible coordination of a catalyst poison to an active organometallic complex is likewise responsible for an altered catalyst concentration in solution. Inhibition of catalyst turn over may be determined by too strongly coordinating substrates, products, anions and solvents, either polar or aromatic. Deactivation phenomena are especially relevant for industrial applications: trace impurities in the substrate can have huge effects on activity at the very high substrate to catalyst ratio required for the convenient use of very expensive catalysts.

Generation of the catalytically active species generally requires the release of a weakly coordinating ligand to allow coordination of the incoming substrate. The ensuing temporary coordination unsaturation may lead to aggregation phenomena and formation of polynuclear species which are usually catalytically inactive. In most cases these processes are reversible: to which extent they will influence the overall kinetics of the catalyzed process depends on the magnitude of their equilibrium constants.

Nature itself relies on activation and deactivation phenomena to adjust enzyme biocatalytic activity. In the course of evolution, two possibilities were established to this purpose. On the one hand, the concentration of the enzyme can be altered, which is determined by the rates of formation and decomposition within the cell. Alternatively, the enzyme itself can be altered in order to control its activity. This is mainly achieved by cooperative (in enzymes with multiple binding sites, the binding of the first substrate molecule influences the ability of the following substrate molecule to bind) and allosteric (regulation of the active site through the binding of a ligand to a second regulatory site, other than the active site) interactions.[3] The feedback inhibition of aspartate transcarbamoylase is an archetypal example of allosteric modulation for the fine control of metabolic enzyme reactions.

Control over the activity of functional enzymes may be achieved by reversible inhibition which results in a temporary reduction of enzyme activity. Inhibitors differ in the mechanism by which they decrease enzyme activity, either competitive, uncompetitive or mixed. For the simple Michaelis-Menten kinetics the principle of reversible inhibition is shown in Scheme 1.

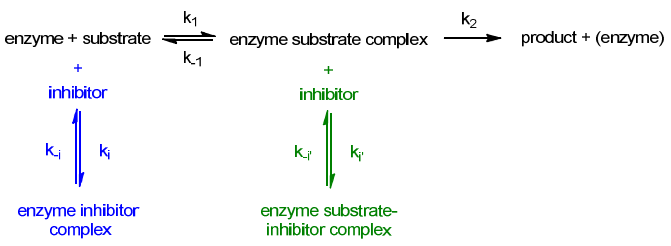

Scheme 1 Competitive (blue), uncompetitive (green) and mixed (blue and green) inhibition in enzyme catalysis.

In case of competitive inhibition, the inhibitor binds at the catalytic active site of the free enzyme thus preventing the substrate to coordinate. An uncompetitive inhibitor does not bind to the enzyme but to the enzyme substrate complex. Sequestration of the enzyme substrate complex by the inhibitor will reduce the macroscopic activity. A special case of uncompetitive inhibition is the inhibition by the substrate itself. Known is also a mixed inhibition.

By kinetic analysis using different inhibitor concentrations it is possible to discriminate among the three cases.[3]

Two excellent books have dealt with the topic of homogeneous catalyst activation, deactivation and stability.[4] The present work is intended to provide an up-dated overview of possible activation and deactivation phenomena in homogeneous catalytic processes promoted by different types of *rhodium complexes* containing *diphosphine ligands*, including more recent results which are not included in the above mentioned references.

2. Induction periods (catalyst 'activation')

The 'active species' mediating a catalytic process are characterized by their high reactivity, which render them fleeting and difficult to characterize. They are generated from suitable catalyst precursors which are more stable, possess a longer shelf life and are therefore easier to handle. The catalyst precursor usually contains labile ligands which can be easily displaced to afford free coordination sites available for incoming substrates. The classical example is the Wilkinson catalyst [$RhCl(PPh_3)_3$]: the catalytic active species is a 14-electron complex which arises from the 16-electron complex through dissociation of one triphenylphosphine PPh_3.[5] Typical, so-called 'spectator ligands'[6] such as cyclic diolefins, like cod (1,5-cyclooctadiene) or nbd (2,5-norbornadiene), ethylene and CO can also stabilize the active catalysts leading to *precatalysts (precursors)*.

Thus, in many cases the actual catalyst, whose true nature often remains undisclosed, is generated from the precatalyst through a *preactivation (preformation, incubation)* process. In some instances, this requires the presence of a *cocatalyst* which is itself inactive. The Ziegler-Natta polymerization promoted by Ti- or V-based catalysts with MAO (*m*ethyl*a*lumin*o*xan) as cocatalyst is a typical example on industrial scale.[4a,7]

The application of precatalysts or their formation by the *in situ* technique is another very common approach to perform catalytic reactions. Neutral rhodium complexes of the type [Rh(diphosphine)(μ_2-Cl)]$_2$, which are used as precatalysts for a plethora of diverse catalytic processes (see section 6), are often generated *in situ* from the corresponding diolefin complexes and the desired diphosphine. The resulting solution is used directly for catalysis. The fact that the free diolefin is still present and can therefore act as a competing coordinating ligand to the metal, thus affecting the catalyst activity, at least in the early stages of the reaction, is often overlooked.

Figure 2 shows the differences in hydrogen up-take as a function of time in the asymmetric hydrogenation of a β-dehydroamino acid derivative promoted by the rhodium-Et-DuPHOS catalyst (Et-DuPHOS = 1,2-bis(2,5-

diethylphospholano)benzene) in methanol when using the active catalyst, (red curve), the commercial available precatalyst (green) and the catalyst generated *in situ* by reaction of the cationic cod precursor and the chiral ligand (blue curve).[8]

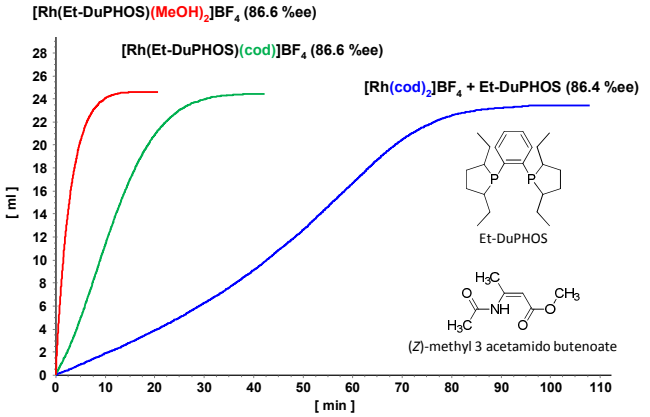

Figure 2 Hydrogen up-take as a function of time in the hydrogenation of (*Z*)-methyl 3-acetamido butenoate (1.0 mmol) with the rhodium-Et-DuPHOS catalyst in 15.0 mL methanol, at normal pressure and 25°C using different catalyst sources: 0.01 mmol $[Rh(cod)_2]BF_4$ + 0.01 mmol Et-DuPHOS (*in situ*, blue curve), 0.01 mmol $[Rh(Et\text{-}DuPHOS)(cod)]BF_4$ (green curve) and 0.01 mmol $[Rh(Et\text{-}DuPHOS)(MeOH)_2]BF_4$ (red).

Distinct *induction periods* are evident for both the case of $[Rh(Et\text{-}DuPHOS)(cod)]BF_4$ and the *in situ* generated catalyst, i.e. the hydrogenation accelerates in the initial stages of the reaction, as more of the catalytic active species $[Rh(Et\text{-}DuPHOS)(MeOH)_2]BF_4$ is being generated in the 'activation' phase as shown in Scheme 2.

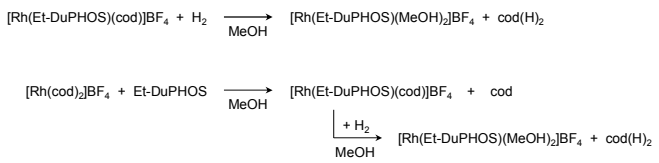

Scheme 2 Generation of the catalytically active species $[Rh(Et\text{-}DuPHOS)(MeOH)_2]BF_4$ from the commercially available precatalyst $[Rh(Et\text{-}DuPHOS)(cod)]BF_4$ and the catalyst generated *in situ* by reaction of the cationic cod precursor $[Rh(cod)_2]BF_4$ and the chiral ligand Et-DuPHOS.

These induction periods, which have been recognized, at least qualitatively, for a long time[9] cause a maximum in the rate profile (a detailed kinetic treatment of the *in situ* case reported in Figure 2 is to be found in reference [4b]). It should be noted that enantioselectivity is not affected by the different methods used for catalyst preparation.

Systematic NMR investigations into the asymmetric hydrogenation of methyl (*Z*)-*N*-acetylamino cinnamic acid (mac) with the system rhodium-Et-DuPHOS (1,2-bis(2,5-dimethyl-phospholanyl)benzene) and (*Z*)-methyl-*N*-benzoylaminocinnamate with rhodium-DIPAMP (1,2-bis-(o-methoxy-phenyl-phenyl-phosphino)-ethane) under stationary conditions ('in operandi')[10] have shown that, during the reaction under normal hydrogen pressure at about room temperature, hydrogenation of the substrate is faster than that of cod in the catalyst precursor $[Rh(diphosphine)(cod)]BF_4$, a not negligible part of which, in both cases *circa* 50%, is still unconverted when substrate hydrogenation is complete.[11] Therefore the use of the cod catalyst precursors is not economical.

Removal of cod in the catalyst precursor by means of hydrogenation frees the coordination sites required for binding of the substrate. Hydrogenation of cod is slower than that of the substrate but the two proceed parallel. The amount of active catalyst available for catalysis increases over time. This is macroscopically manifested in the increase of reaction rate in the early stages of the reaction and thus in the presence of an induction period.

Several factors affect the induction period: the diolefin (its concentration (Figure 2) and the stability of the corresponding diolefin rhodium complex), the prochiral olefin (its concentration and the stability of the corresponding rhodium substrate complex), the solvent and the temperature.
Hydrogenation of cod is slower than that of nbd so longer inductions period are expected for cod containing catalyst precursors (Table 1). Yet, when the concentration of the substrate is very high and the catalyst loading very low (i.e. substrate / catalyst = 10 000), as required by industrial applications, induction periods become more and more negligible compared to the overall time required for complete substrate conversion and differences between the two catalyst precursors become difficult to appreciate. This could be proved in the hydrogenation of dimethyl itaconate with the rhodium-Me-DuPHOS catalyst.[12] Competition experiments in which the hydrogenation of the prochiral olefin was carried out at very high substrate to catalyst ratios using equimolar amounts of cod and nbd rhodium precursors having ligands of *opposite chirality*, afforded an almost racemic product (ee < 3 %), indicating that the amount of substrate converted *during* the induction period, when the two catalysts precursors afford different amounts of enantiomeric catalytically active species, is *relatively* small, although the very low amount of the excess enantiomeric product, 3 %, is not negligible based on the *absolute* product amount (911 mg over 30 g in the example reported above). In order to avoid undesirable induction periods and benefit from the full activity expected for the amount of 'catalyst' added to the reaction vessel, it is advisable to use solvent complexes having the general formula [Rh(diphosphine)(solvent)$_2$]anion: they are prepared by pre-hydrogenation of the corresponding diolefin complexes in the absence of the prochiral olefin. Solvent complexes are also better suited for kinetic investigations.

While several solvent complexes with different diphosphine ligands have been characterized by ^{31}P NMR spectroscopy, only recently have the first X-ray structures of such reactive species been published.[13] In Figure 3, the molecular structures of complexes $[Rh(BINAP)(MeOH)_2]BF_4$ (BINAP = (2,2'-bis(diphenylphosphino)-1,1'-binaphthyl) and $[Rh(Synphos)(acetone)_2]BF_4$ (Synphos = 6,6'-bis(diphenyl-phosphino)-2,2',3,3'-tetrahydro-5,5'-bi-1,4-benzodioxin) are presented.

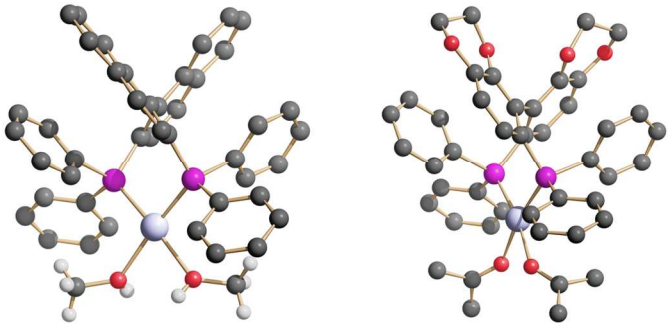

Figure 3 Molecular structures of the cations of $[Rh(BINAP)(MeOH)_2]BF_4$ (left) and $[Rh(Synphos)(acetone)_2]BF_4$ (right). Hydrogen atoms (except these on the methanol) are omitted for clarity.

Several methods have been reported in the literature which allow, under *isobaric* conditions, to measure the pseudo 1[rst] order rate constant ($k_{2diolefin}$) for the diolefin hydrogenation en route to the solvent complexes.

In principle it is possible to track either the *stoichiometric* hydrogenation (by measuring the hydrogen uptake[14a] with ^{31}P NMR[14b] or UV-Vis spectroscopy[14c] or the *catalytic* reaction in the presence of an excess of the diolefin[14d] under several pressure regimes.[11a] It is likewise possible by means of ^{1}H NMR to assess the H_2 concentration in solution during diolefin hydrogenation under *isochoric* conditions.[15] Through on-line automatic recording of hydrogen consumption and subsequent parameter optimization using a *suitable* kinetic model, it is likewise possible to determine the pseudo rate constant for diolefin hydrogenation.[16]

An overview of the issues concerning diolefin hydrogenation (cod and nbd) and a list of related rate constants for 24 rhodium-diphosphine complexes are to be found in reference [4b]. Additional values which have been published so far are collected in Table 1.

Similar data have been published for monodentate phosphines ($[Rh(MonoPhos)_2(nbd)]BF_4$,[17a] $[Rh(MonoPhos)_2(cod)]BF_4$,[17b] ($[Rh(PPh_3)_2(cod)]BF_4$.[17c]

Table 1 Pseudo rate constants ($k_{2diolefin}$)[18] for the hydrogenation of cod and nbd for different [Rh(diphosphine)(diolefin)]anion complexes (25.0 °C; 1.013 bar total pressure) The values were obtained in methanol as solvent and with BF_4^- as anion unless stated otherwise, see special conditions.

Ligand	special condition		$k_{2\,COD}$ (1/min)	$k_{2\,NBD}$ (1/min)	$k_{2\,NBD}$ / $k_{2\,COD}$	reference
DPPE			$3.3\cdot10^{-3}$	$1.7\cdot10^{1}$	5300	11a,14c
DIPAMP	MeOH		ca. $2.9\cdot10^{-3}$	ca. $9.0\cdot10^{0}$	ca. 3100	19
	EtOH		-	$1.3\cdot10^{1}$		
	i-PrOH		-	$5.9\cdot10^{0}$		
	THF		-	$5.0\cdot10^{0}$		
	trifluoroethanol		-	$3.9\cdot10^{0}$		
	propylene carbonate		-	$4.8\cdot10^{0}$		
	MeOH [a]		$3.4\cdot10^{-3}$			15
3-Pen-SMS-Phos				$3.8\cdot10^{0}$		20
Me-DuPHOS	MeOH		$1.2\cdot10^{-2}$	$3.5\cdot10^{1}$	ca. 300	14c
	THF		$1.6\cdot10^{-2}$	$3.9\cdot10^{1}$	ca. 250	
	propylene carbonate		$1.4\cdot10^{-2}$	$1.8\cdot10^{1}$	ca. 130	
Et-DuPHOS	MeOH		$2.8\cdot10^{-2}$ [b]	$5.2\cdot10^{1}$	ca. 2000	14c
	acetone		$3.2\cdot10^{-2}$	-	-	21
	MeOH [a]		$2.3\cdot10^{-2}$			15
CatASium®	MeOH		$5.0\cdot10^{-2}$	$2.5\cdot10^{1}$	ca. 500	14c
	THF		$1.5\cdot10^{-1}$	$1.2\cdot10^{1}$	ca. 80	
	propylene carbonate		$8.5\cdot10^{-2}$	$9.4\cdot10^{0}$	ca. 110	
R-ButiPhane			stoichiometric / catalytic hydrogenations			22
	R = Me		$1.5\cdot10^{-1}$ / $1.0\cdot10^{-1}$			
	R = Et		$3.1\cdot10^{-2}$ / $2.9\cdot10^{-2}$			
	R = 2-propyl		$9.0\cdot10^{-3}$ / $1.0\cdot10^{-2}$			
Tangphos			$3.8\cdot10^{-1}$	$1.9\cdot10^{2}$	ca. 500	23
^{t}Bu-BisP*			$2.1\cdot10^{-1}$	$9.0\cdot10^{1}$	ca. 450	23
BINAP	MeOH	BF_4^-	$2.3\cdot10^{-1}$	$2.7\cdot10^{1}$	ca. 120	14c
		TfO^-	$2.3\cdot10^{-1}$	$2.7\cdot10^{1}$	ca. 120	24
		$BArF^-$	$2.2\cdot10^{-1}$	-	-	
	THF	BF_4^-	$2.8\cdot10^{-1}$	$2.0\cdot10^{1}$	ca. 73	14c
	propylene carbonate	BF_4^-	$1.4\cdot10^{-1}$	$1.7\cdot10^{1}$	ca. 120	
		TfO^-	$1.4\cdot10^{-1}$	ca. $1.5\cdot10^{1}$	ca. 110	24
		$BArF^-$	$1.5\cdot10^{-1}$	-	-	
Synphos			$8.0\cdot10^{-1}$	$6.7\cdot10^{1}$	ca. 80	13a

[a] isochoric conditions. [b] newly measured.

The results show that, regardless of the diphosphine ligand, the hydrogenation of cod is always slower than that of nbd, meaning a longer induction period. Therefore the very small pseudo rate constants observed for the ligands DPPE (1,2-bis(diphenylphosphino)ethane) and DIPAMP imply that for the complete hydrogenation of cod in methanol at room temperature and normal pressure 24 and 30 hours are necessary respectively with the two ligands! This confirms previous findings concerning the challenging quantitative hydrogenation of cod[25]: Failure to recognize these rather long induction periods may lead to underestimation of the 'real' efficiency of the corresponding rhodium-diphosphine catalyst in the hydrogenation of specific substrates, especially in relation to the application of high throughput methods in catalyst testing.[26] The pseudo rate constants are not affected by the counteranion in the catalyst precursor (Refer to Table 1, BINAP).

According to the data reported so far, the hydrogenation of the diolefin is clearly slower than that of the prochiral olefin. This is not always the case. Hydrogenation of mac with the rhodium-BINAP catalyst is slower than that of cod.[24] In this case nearly no induction period is observed.

The positive influence on activity arising from the use of the solvent complex as compared with the diolefin complex has been described also in the case of reductive amination.[27] Selectivity changes as well in this case, often an indication that other phenomena come into play, see section 4.2.

To summarize, depending on the experimental conditions, the conversion of frequently applied precatalysts into active species may be associated with the observation of an induction period. This is due to the parallel hydrogenation of both the diolefin in the rhodium precatalyst (slow) and the prochiral substrate olefin (fast), whereby an apparent 'activation' of the catalyst is to be observed. In reality this reflects the increasing availability of the active species as more of it is being formed through conversion of the applied rhodium-diolefin complex.

3. Catalyst deactivation due to formation of non-reactive, monomeric species

The product of a homogeneously catalyzed reaction is formed as a result of chemical events taking place within the coordination sphere of the metal: substitution of the product molecule in the catalyst product complex in the final step of the catalytic cycle is, in most cases, possible and this ensures that a new molecule of the substrate may displace it and coordinate to the catalyst to start a new catalyst turn over. If the reaction solution contains species which are able to coordinate to the metal, such species – inhibitors - compete with the substrate and may hamper access of the latter to the catalyst, as exemplified by the blue equilibrium presented in Scheme 1. The net result is a reduction of the amount of catalyst available for the process of interest, which manifests itself in a macroscopic reduction of activity.

For example, aromatics are typical inhibitors for the catalytically active solvent complexes [Rh(diphosphine)(solvent)$_2$]anion. They form stable complexes, a phenomenon which has long been known.[28] Such complexes can be unambiguously identified by means of ^{103}Rh NMR spectroscopy.[29] Compared to those of the corresponding solvent complexes their signals are shifted to higher field: the chemical shifts additionally show the dependence from the size of the chelated ring formed by the coordinated diphosphine.[30] ^{1}H and ^{13}C NMR data provide further evidence of the presence of a π-arene complex. In the case of [Rh(Et-DuPHOS)(η^6-benzene)]BF_4, the signals of the coordinated benzene are shifted to higher field by 0.75 ppm in the ^{1}H and 27.8 ppm in the ^{13}C spectrum. The coupling constants are $^{1}J(^{13}C,^{103}Rh)$ = 2 Hz and $^{1}J(^{13}C,^{1}H)$ = 174 Hz, the latter being typical of an π-arene complex.[31]

In Figure 4 the X-ray structures of complexes [Rh((*R,R*)-Et-DuPHOS)(η^6-benzene)]BF_4 and [Rh((*S,S*)-Me-DuPHOS)(η^6-toluene)]BF_4 are shown.[32]

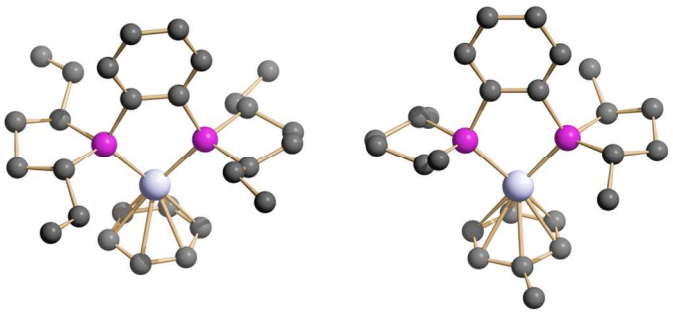

Figure 4 Molecular structure of the cations [Rh((*R,R*)-Et-DuPHOS)(η^6-benzene)]BF_4 (left) and [Rh((*S,S*)-Me-DuPHOS)(η^6-toluene)]BF_4 (right). Hydrogen atoms are omitted for clarity.

Surprisingly heteroarenes do not bind through the heteroatom but rather adopt π-arene coordination. Examples of such coordination are shown in Figure 5 where the X-ray structures of [Rh((*R,R*)-Me-DuPHOS)(η^6-aniline]BF_4 and [Rh(DPPF)(*N*-methyl-η^6-aniline)]BF_4 (DPPF = 1,1'-Bis(diphenylphosphino)ferrocene) are presented.[33]

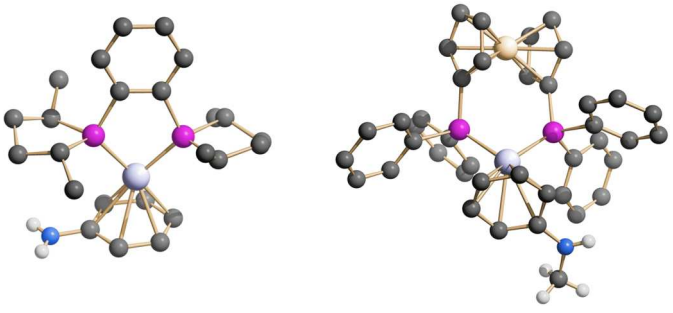

Figure 5 Molecular structure of the cation [Rh((*R,R*)-Me-DuPHOS)(η^6-aniline)]BF_4 (left) and [Rh(DPPF)(*N*-methyl-η^6-aniline)]BF_4 (right). Hydrogen atoms (except these on the amino and amino methyl group) are omitted for clarity.

3. 1. Deactivation by the solvent

Typical solvents for homogeneous hydrogenations are simple alcohols, tetrahydrofurane, and aromatics such as toluene or benzene. Mixtures of an alcohol and an arene have also been used as solvent for asymmetric hydrogenations.[34]

Aromatics can coordinate to rhodium-diphosphine complexes giving rise to species having general formula [Rh(diphosphine)(η^6-arene)]anion. The resulting 18-electron species are coordinatively saturated and relatively stable, to the point that aromatics may represent potential inhibitors, a fact quite often overlooked. Arenes can adopt also an η^4-coordination mode: the resulting electronically unsaturated metal arene π-complexes may therefore still be able to bind the incoming substrate.[35]

Articles reporting on the inhibiting effect of an aromatic solvent in asymmetric hydrogenation are therefore scarce. The asymmetric hydrogenation of ethyl 2-(benzoyloxy)crotonate catalyzed by a cationic rhodium-Et-DuPHOS complex proceeds with very good activity and selectivity in non-aromatic solvents but does not occur in benzene.[36] The formation of the stable benzene complex [Rh((*R,R*)Et-DuPHOS)(η^6-benzene)]$^+$, Figure 4 left, has been put forward as the cause of inactivity.

When hydrogenation of (*Z*)-methyl-3-acetamido butenoate with the rhodium-Me-DuPHOS system is carried out in toluene at ambient temperature under 20 bar hydrogen pressure using the *in situ* prepared catalyst, complete conversion requires 24 h and affords an ee-value of 63.7 %.[37] The hydrogenation of the same substrate in methanol using the active catalyst [Rh(Me-DuPHOS)$(MeOH)_2$]BF_4 is complete within 4 min under normal pressure and room temperature with an ee-value of 87.8 %.[38] The different behavior is simply caused by the deactivating effect of the aromatic solvent in the first case as a large amount of the metal is sequestered as stable and inactive π-arene complex, Figure 4, right. Instead, in methanol the total amount of rhodium introduced as solvent complex [Rh(Me-DuPHOS)$(MeOH)_2$]BF_4 is catalytically active in the asymmetric hydrogenation.

In the presence of aromatics - the latter are often an impurity in solvents like methanol - how much of the total rhodium concentration [Rh_0] is in the form of the arene complex [Rh_{arene}] can be calculated by solving the following equation 1:[33a]

$$[Rh_{arene}] = \frac{[Rh_0]}{\left(\frac{K_{substrate}}{K_{arene}}\cdot\frac{[substrate]}{[arene]}\right)+1} \quad (1)$$

$$K_{substrate} = \frac{[substrate\ complex]}{[solvate\ complex]\cdot[substrate]}$$

$$K_{arene} = \frac{[arene\ complex]}{[solvate\ complex]\cdot[arene]}$$

It is evident that the extent of inhibition depends not only on the stability of the arene complex as quantified by K_{arene} but also on the stability of the catalyst substrate complex ($K_{substrate}$) and the free concentrations of the substrate and arene.

The stability constants for the formation of [Rh(DPPE)(mac)]$^+$ and [Rh(DPPE)(η^6-toluene)]$^+$ from the solvate complex [Rh(DPPE)$(MeOH)_2$]$^+$are K'_{mac} = 5300 L/mol[39] and $K'_{toluene}$ = 97 L/mol[40] respectively. By introducing these values in Eq. 1 it is possible to calculate the relative amounts of the two species in solution. Assuming a total rhodium concentration of c_0 = 0.0125 M (0.01 mmol) and a 1:10 catalyst-substrate ratio in a solvent mixture consisting of 0.6 mL methanol and 0.2 mL toluene, 26 % of the rhodium present in solution is blocked as inactive arene complex [Rh(DPPE)(η^6-toluene)]$^+$, which is in good agreement with the integration data extracted from the ^{31}P NMR spectrum (29 %) of the solution, Figure 6. In pure toluene (0.8 mL), under otherwise identical conditions, the relative concentration of [Rh(DPPE)(η^6-toluene)]$^+$ would rise to 58 % despite the fact that its stability constant is 50 times lower than that of [Rh(DPPE)(mac)]$^+$.

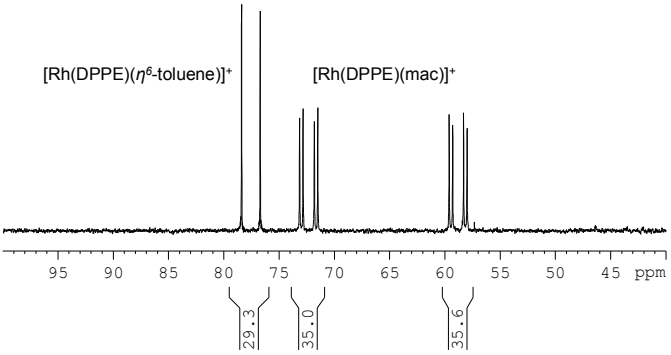

Figure 6 ^{31}P NMR spectrum of the solution prepared by dissolving [Rh(Me-DuPHOS)$(MeOH)_2$]BF_4 (0.01 mmol), mac and toluene (1 : 10 : 200) in 0.6 mL methanol.

Upon addition of methyl 2-acetoamidoacrylate, a benchmark substrate in asymmetric hydrogenation, to a solution of [Rh(Et-DuPHOS)(η^6-benzene)]$^+$ in a non-coordinating solvent like dichloromethane, the catalyst substrate complex is built up together with free benzene. This proves that the formation of the arene complex is reversible[36] and therefore asymmetric hydrogenation is indeed possible in aromatic solvents but a decrease in activity should be taken into account.[37,41]

Unfortunately there are less data available concerning the stability constants of cationic rhodium arene complexes[40,42,43] than for catalyst substrate complexes[39,40,42a] and therefore this kind of calculation is not always possible.

Even the kinetics of (prochiral) substrate hydrogenation is influenced by the formation of the arene complex. When the stability constant of the catalyst substrate complex is very low (reaction 1^{rst} order in substrate concentration, like for example in the case of the system [Rh(Ph-ß-glup-OH)$(MeOH)_2$]BF_4 / dimethyl itaconate (Ph-ß-glup-OH = 2,3-bis(*O*-diphenylphosphanyl-*ß-D*-glucopyranoside) in methanol at room temperature and normal pressure), only the poisoning arene can compete with the largely in excess solvent for the metal. If, on the other hand, the catalyst-substrate complex is very stable (reaction 0th order in substrate concentration, like for example in the case of the system [Rh(DIPAMP)$(MeOH)_2$]BF_4 / (*Z*)-*ß*-

(*N*-Acetyl)-aminocrotonic acid methyl ester in methanol at room temperature and normal pressure) then the substrate can effectively compete with the inhibiting arene for the metal.[32] In the first case, the reaction remains 1st order in the substrate concentration even in the presence of inhibitors (the reaction will only be slower), the presence of which is therefore quite difficult to recognize. In the second case a continuous decrease in activity is observed instead because the concentration of the inhibitor remains constant during the reaction while that of the prochiral olefin diminishes with increasing conversion. Hence an important (tacit) assumption of the formal kinetic treatment of catalysis, that the active catalyst concentration is constant, is no longer valid.

3. 2. Deactivation by the substrate / product

Even substrates / products having phenyl rings in their structure, a feature common to plenty of unsaturated molecules tested in (asymmetric) hydrogenation, are able to form stable rhodium arene complexes.

By systematic investigation into the asymmetric hydrogenation of mac promoted by the precatalyst [Rh(*t*Bu-BisP*)(nbd)]BF_4 (*t*Bu-BisP* = 1,2-bis(*tert*-butylmethylphosphino)ethane) it was possible to detect diastereomeric dinuclear complexes in which the substrate acts as a bridging ligand between two rhodium centres: to one it is coordinated through the double bond and the oxygen of the amido group, as expected for this kind of substrates, to the other one in a η^6 fashion through its phenyl ring, Figure 7 left shows the resulting species which is stable even at room temperature. This is likely the result of the reaction between the catalyst substrate complex and the solvent complex in the presence of a relative low amount of the substrate.[43] The displacement of solvent molecules from the solvent complex through coordination of the phenyl ring in the substrate bound to another rhodium centre obviously affords a thermodynamically more stable system.

The complex [Rh(*t*Bu-BisP*)(η^6-macH_2)]BF_4, in which the hydrogenation product of mac coordinates to the metal through its phenyl ring, could be detected by NMR spectroscopy.[43] Likewise the η^6-arene complexes of the hydrogenated phenylenamide and *p*-chlorophenylenamide, Figure 7 right, could be spectroscopically identified at –100 °C.[44]

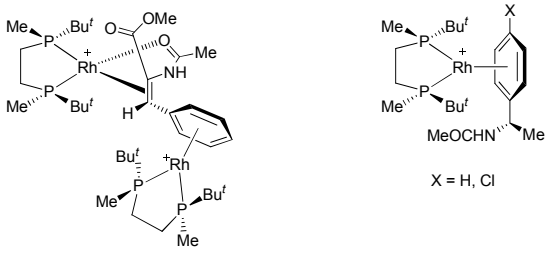

Figure 7 Stable η^6-arene complexes arising from the reaction of substrate mac (left) and hydrogenation product (right) with the catalytically active solvent complex [Rh(*t*Bu-BisP*)$(MeOH)_2$]$^+$.

Arene complexes of hydrogenation products were detected during the hydrogenation of styrene derivatives promoted by rhodium catalysts containing the ligands DPPB and Josiphos.[45] Although such product complexes had been known for a long time in relation to triphenylphosphine iridium complexes, also with regard to their deactivating effects,[46] the detection of the rhodium η^6-product complexes, present in very low concentration, was only possible by taking advantage of the large signal enhancement offered by PHIP (*p*ara *h*ydrogen *i*nduced *p*olarisation) NMR spectroscopy.

Very recently the X-ray structures of both substrate and hydrogenation product complexes [Rh((*S,S*)-Et-DuPHOS)(vinyl-η^6-benzene)]BF_4 and [Rh((*S,S*)-Et-DuPHOS}(ethyl-η^6-benzene)]BF_4 were published, Figure 8.[21]

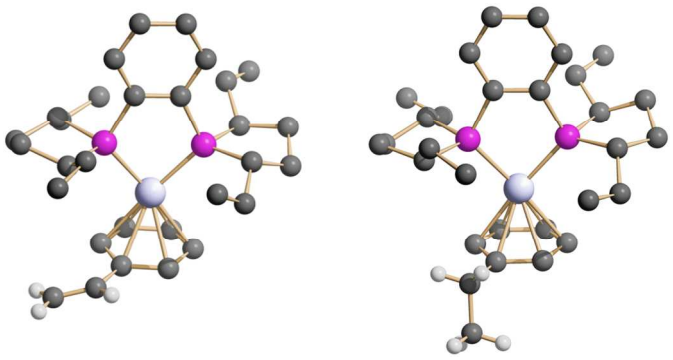

Figure 8 Molecular structures of the cations of [Rh((*S,S*)-Et-DuPHOS)(vinyl-η^6-benzene)]BF_4 (left) and [Rh((*S,S*)-Et-DuPHOS)(ethyl-η^6-benzene)]BF_4 (right). Hydrogen atoms (except these on the vinyl and ethyl group) are omitted for clarity.

In the following chapter it will be shown that such complexes can play a pivotal role in the deactivating of Rh complex catalyzed reactions.

3. 3. Deactivation by polystyrene resins as matrix for catalyst heterogenisation

The anchoring of molecularly well-defined rhodium complexes on solid support allows to combine the advantages of homogeneous catalysis (high activity and selectivity) with the benefit of catalyst recycling offered by heterogeneous catalysis. However one main drawback of this approach to the economical use of precious and expensive catalysts is the possibility of metal leaching from the solid support into the solution.

Heterogenization of cationic rhodium complexes of general formula [Rh(diphosphine)$(solvent)_2$]anion can be achieved through proper modification of either the diphosphine ligand or the counteranion so that it can be attached to a polystyrene resin and thus allow anchoring of the catalyst complex onto the solid support. However, during this process, part of the metal can be 'scavenged' by the resin through formation of η^6-arene complexes, which will affect the activity and/or selectivity of the desired process. In order to prove this possibility, soluble polystyrene standards like PS4000 (38 monomers) or PS30000 (288 monomers) were added to a solution of [Rh(Et-

DuPhos)(THF-d_8)$_2$]BF_4, in deuterated tetrahydrofuran: the formation of η^6-arene complexes with the soluble polysterene was corroborated by the dramatic change in the ^{103}Rh chemical shift of the resulting complex in solution to –1071 ppm, compared to –38 ppm in the solvent complex.[21] Additional NMR data and the stability constants of η^6 (poly)-styrene complexes are collected in Table 2.

The equilibrium constants for the rhodium-η^6-arene complexes in acetone were determined by UV-vis spectrometric titration of the free and coordinated (poly)styrene, Table 2.[47] The stability of the complexes decreases in going from styrene to polystyrene and with increasing molecular weight of the latter, because of the greater steric hindrance caused by the longer polymer chain. Yet the stability constants of the η^6-arene complex with a polymer consisting of 288 monomeric units is of the same order of magnitude of the η^6-benzene rhodium-DPPE complex.[40]

Table 2 ^{31}P and ^{103}Rh NMR chemical shifts, coupling constants J(^{31}P,^{103}Rh) and stability constants for selected rhodium-η^6-(poly)styrene complexes as compared to the corresponding solvent complexes [Rh(Et-DuPhos)(L$_x$)]BF_4 (MeOH, THF x = 2; (poly)styrene x = 1).

L	^{31}P ppm	J(^{31}P,^{103}Rh) Hz	^{103}Rh ppm	solvent	stability constant L / mol in aceton
MeOH	94.9	206	–151	MeOH-d_4	
THF	96.1	207	–38	THF-d_8	
styrene	92.2	202	–1011	MeOH-d_4	107
PS4000 38 monomers	93.2	≈ 203	–1073	acetone-d_6	42
PS30000 288 monomers	93.4	≈ 203	–1047 to –1063	acetone-d_6	17
	92.9	≈ 200	–1071	THF-d_8	

If, during the preparation of the heterogeneous catalyst, part of the rhodium is not bound to the resin in the desired form (neither covalent nor ionic) but as η^6-coordinated arene complex, then the latter is in equilibrium with the solvent complex (Scheme 3) and can be washed out from the resin when the resin is rinsed with the solvent after catalyst loading and recycling.

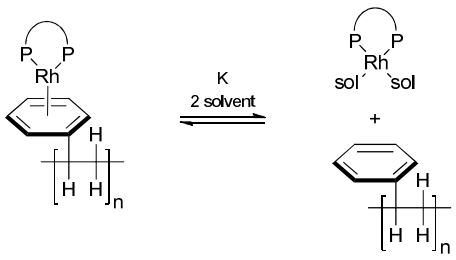

Scheme 3 Equilibrium reaction between the η^6-polymer coordinated rhodium-diphosphine complex and the solvent diphosphine rhodium complex.

3. 4. Deactivation by additives

Additives having aromatic structural features can likewise cause a decrease in the activity of the rhodium catalyst by formation of η^6-arene complexes.

The hydrogenation of prochiral organic substrates like itaconic acid and dimethyl itaconate, becomes possible in aqueous solution in the presence of surfactants like SDS or Triton X-100, Figure 9: under suitable conditions, the surfactant monomers aggregate to form micelles that are soluble in water while having an hydrophobic core within which the catalytic reaction takes place. The precious catalyst, which is confined into the micelles, can be recycled by membrane ultrafiltration.[48]

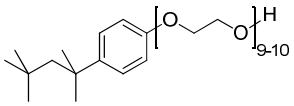

Figure 9 Stucture of the non-ionic surfactant Triton X-100.

For the rhodium-BPPM / dimethyl itaconate system (BPPM = 1-tert-butoxycarbonyl-4-diphenylphosphino-2-(diphenylphosphinomethyl)-pyrrolidine) it was possible to show that the TOF decreases when the Triton X-100 concentration is increased. Selectivity is unaffected and an enantiomeric excess of 60 % as in methanol is achieved. A broad doublet is observed at 97.3 ppm in the ^{31}P NMR spectrum with a Rh-P coupling constant of 204 Hz (Figure 10): this signal correlates with a singlet in the ^{103}Rh NMR spectrum at -1006 ppm indicating the formation of a new η^6-arene complex. Further unambiguous characterization comes from ^{1}H NMR (the signals for the hydrogens of the coordinated arene are shifted to higher field than expected for the free arene: 7.17, 6.98, 6.37, and 6.05 ppm).

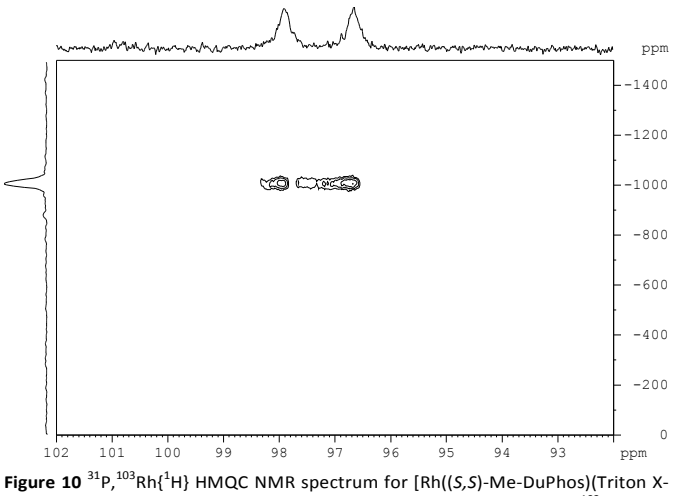

Figure 10 ^{31}P,^{103}Rh{^{1}H} HMQC NMR spectrum for [Rh((*S,S*)-Me-DuPhos)(Triton X-100)]BF_4 in methanol-d$_4$, taken at 317 K. The chemical shift δ of the ^{103}Rh NMR signal (–1006 ppm) is within the range of known Rh-arene complexes.

The examples reported so far show that, because of the possibility of the formation of η^6-arene complexes and because of their non-negligible stability, care should be taken when evaluating the activity of rhodium diphosphine catalysts in

processes which may involve 'arene sources' like solvent, substrate / product, additives, polystyrene solid supports or impurities. The possible resulting η^6-arene complexes are coordinatively saturated 18-electron species which cannot coordinate incoming substrates or undergo oxidative addition and are consequently catalytically inactive. The formation of such species is however reversible: the extent of inactivation is determined by the concentration of competing complexing agents present in solution which might displace the coordinated arene and by the ratio of the stability constants of the corresponding rhodium complexes.

4. Catalyst deactivation due to formation of multinuclear complexes

4.1. Dinuclear complexes

The dimerization of the solvate complex $[Rh(DPPE)(MeOH)_2]BF_4$ to yield $[Rh(DPPE)]_2^+$ was described for the first time in 1977.[40] In the dimer each DPPE acts as a bridging ligand between the two rhodium centres: it is chelated to one metal through the phosphorus donors, it is coordinated to the second one though one of the phenyl substituents on the phosphorus. Such dimers have found application as catalyst precursors, for example in hydroacylation,[49] the intramolecular cyclization of 4-pentenals to cyclopentanones. Other dimeric rhodium diphosphine complexes, featuring a similar coordination pattern which of course, is available only when the diphosphine ligand contains phenyl rings, have been described,[50] also for monodentate phosphine ligands.[Error! Bookmark not defined.a,51]

These species are usually generated *in situ* by hydrogenation of a cationic bisdiolefin rhodium complex like, for example, $[Rh(cod)_2]OTf$ and a diphosphine like BINAP, in an unpolar solvent, either dichloromethane or dichloroethane, and used as such for catalysis.[52]

So far, the only ligands for which the X-ray structures of the corresponding dimer rhodium complexes have been reported are DPPE, DIPAMP, BINAP and Synphos. In Figure 11 the molecular structures of the cations of $[Rh((S,S)\text{-DIPAMP})]_2(BF_4)_2$ and $[Rh((S)\text{-Synphos})]_2(BF_4)_2$ are shown.

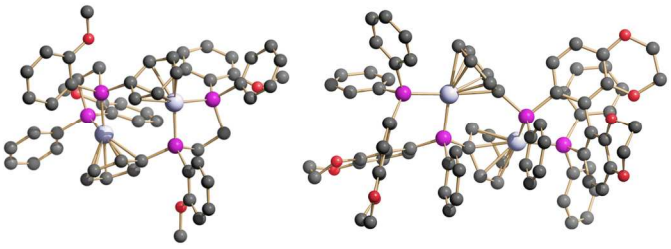

Figure 11 X-ray structures of the cations of $[Rh((S,S)\text{-DIPAMP})]_2(BF_4)_2$ (left) and $[Rh((S)\text{-Synphos})]_2(BF_4)_2$ (right). Hydrogen atoms are omitted for clarity.

Upon coordination to the metal through one of its aryl substituents, one phosphorus atom on each of the two Synphos ligands becomes a stereocentre, whose absolute configuration depends on which of the two diastereotopic phenyl substituents is involved in coordination. The same applies to other aryl substituted diphosphines which act as bridging ligands in the same fashion and in principle different diastereomeric dimers may exist. In the case of DIPAMP, whose phosphorus donors are stereogenic, dimers are built up with the involvement of two phenyl substituents or one phenyl and one *o*-anisyl.[19]

An estimation of the average stability constant of these dimeric species by NMR spectroscopy in methanol has provided a value of ca. 50 L/mol.[19] The dimers are therefore much more stable than previously assumed.[53] In methanol $[Rh(DIPAMP)]_2(BF_4)_2$ coexists in equilibrium with the solvent complex $[Rh(DIPAMP)(MeOH)_2]BF_4$. For BINAP, the equilibrium between solvent complex and dimer is entirely on the side of the solvate complex $[Rh(BINAP)(MeOH)_2]BF_4$.[13b,19] The different stability of the two dimers is clearly due to the different dimensions of the chelate ring formed by the two ligands upon coordination, 5-membered *vs* 7-membered.

The unexpected stability of the aryl-bridged dimers, which in non-polar solvents like dichloromethane is clearly much greater than in polar ones (in non-polar non-coordinating solvents, mononuclear solvent complexes cannot be stabilized) can explain catalyst deactivation and the ensuing reduced activity. The dimers are coordinatively saturated 18-electron species which, in order to coordinate the incoming substrate and start the catalytic cycle, should first dissociate into monomers.

Kinetic investigations into the reductive cyclization of 1,6 diynes promoted by rhodium-BINAP complex[54] in dichloromethane have defined a partial 0 order reaction, both in the substrate and hydrogen concentration.[55] This result can be explained assuming that dissociation of the dimer $[Rh(BINAP)]_2(BF_4)_2$, built up after diolefin hydrogenation in the catalyst precursor, is the rate-determing step of the catalytic process.

4.2. Trinuclear complexes

Addition of a base like triethylamine to the solvate complex $[Rh(DPPE)(MeOH)_2]BF_4$ leads to the formation of a *trinuclear* rhodium complex $[Rh_3(DPPE)_3(\mu_3\text{-}OMe)_2]BF_4$, first reported in 1977.[40] A structural related complex with the ligand BINAP was published later.[56]

In the complex, the three rhodium atoms lie at the vertexes of a regular triangle, each coordinated to a bidentate diphosphine located perpendicular to the Rh_3 plane. Above and below the plane are the two μ_3-bridging anions. Other trinuclear rhodium complexes have been synthesized sharing this structural motif.[57] They are quite stable. X-ray structures have been published for complexes with μ_3-bridging methoxy and/or hydroxy anions and the ligands Me-DuPHOS, DIPAMP, DPPE, *t*-Bu-BisP*, DPPP, BINAP and Synphos,[13a,40,56,57,58] Figure 12 shows two representative examples.

Scheme 3 introduces the general reaction sequence whereby the trinuclear complexes are formed starting from the solvent complex.[59] The base is necessary in order to generate the bridging anions either from the solvent (MeO^-) or from adventitiuos water present in solution (OH^-).

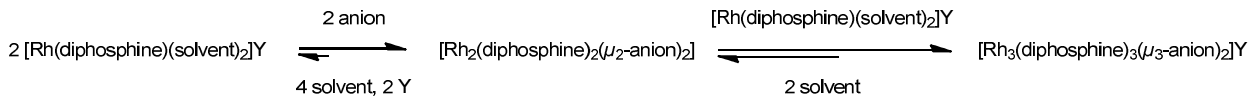

Scheme 3 General reaction sequence for the generation of μ_3-anion bridged trinuclear complexes.

The formation of such trinuclear rhodium complexes can reduce the concentration of rhodium in solution available in the form of catalytically active species and therefore they can be considered a cause for catalyst deactivation, as shown in some cases during asymmetric hydrogenation.[57]

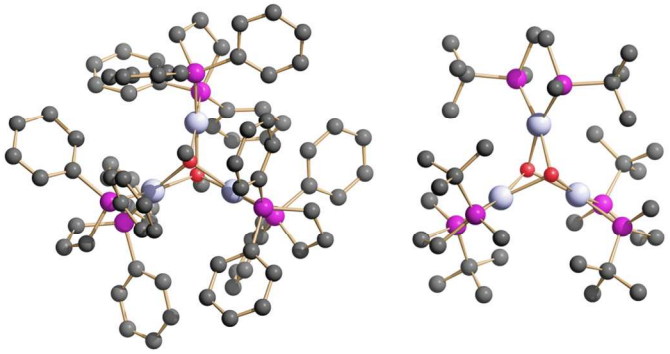

Figure 12 X-ray structures of the cations of $[Rh_3(DPPP)_3(\mu_3\text{-}OMe)_2]BF_4$ (left) and $[Rh_3((R,R)^t\text{Bu-BisP*})_3(\mu_3\text{-}OH)_2]BF_4$ (right). Hydrogen atoms are omitted for clarity.

Interesting, also from a practical point of view, is the fact that the formation of such deactivating trinuclear rhodium complexes can be triggered by substrates which are sufficiently basic, without the need for any added base. The negative effect on activity though might be difficult to recognize. Examples of this type of substrate which have been asymmetrically hydrogenated are (*E*)-1-(2-methyl-3-phenylallyl)piperidine and [2-(3-methoxy-phenyl)-cyclohex-1-enylmethyl]-dimethylamine.[60] When $[Rh(DIPAMP)(MeOH)_2]BF_4$ is added to a solution of the former prochiral olefin in a ratio of 1 : 10 at room temperature, 40 % of the total rhodium content is trapped as catalytically inactive $[Rh_3(DIPAMP)_3(\mu_3\text{-}OMe)_2]BF_4$. When the same catalyst is added to a solution of the second olefin in a ratio 1 : 20, under otherwise identical conditions, then NMR spectroscopy shows that up to 75 % of the total rhodium content is present as $[Rh_3(DIPAMP)_3(\mu_3\text{-}OMe)_2]BF_4$ and, to a minor extent, as $[Rh_3(DIPAMP)_3(\mu_3\text{-}OMe)(OH)]BF_4$.[57]

Halides have also been recognized as possible source of deactivation in reactions catalyzed by rhodium complexes. An example is provided by the asymmetric hydrogenation of 2-methylenesuccinamic acid. The hydrogenation product is a key intermediate in the synthesis of 4-amino-2-(*R*)-methylbutan-1-ol en route towards the receptor antagonist TAK-637. It could be shown that with the catalyst of choice [((*S*,*S*)-Et-DuPHOS)Rh(cod)]BF_4 activity could be increased by a factor of 26 when the substrate was thoroughly purified from chloride containing contaminants.[61] Substrates, which are also relevant for industrial applications, often contain halides as impurities due to incomplete removal during their synthesis. The reduced activity observed in the presence of halides may be ascribed to the formation of recently reported very stable trinuclear rhodium complexes where halides act as μ_3-bridging anions.[58] The molecular structures of $[Rh_3((R,R)^t\text{Bu-BisP*})_3(\mu_3\text{-}Cl)_2]BF_4$ and $[Rh_3((R,R)\text{-Me-DuPHOS})_3(\mu_3\text{-}Br)_2]BF_4$ are presented in Figure 13.

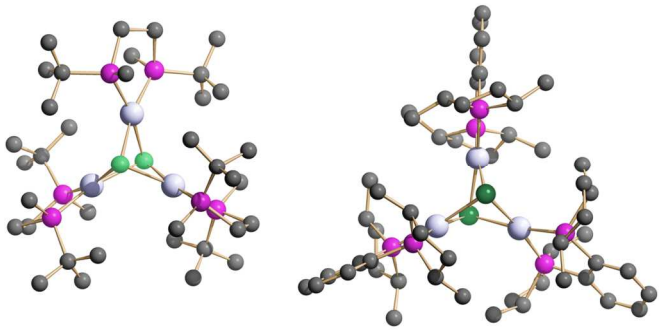

Figure 13 X-ray structures of the cations of $[Rh_3((R,R)\text{-}^t\text{Bu-BisP*})_3(\mu_3\text{-}Cl)_2]BF_4$ (left) and $[Rh_3((S,S)\text{-Me-DuPHOS})_3(\mu_3\text{-}Br)_2]BF_4$ (right). Hydrogen atoms are omitted for clarity.

Such complexes are catalytically inactive as experimentally proved in the asymmetric hydrogenation of mac and dimethyl itaconate with the solvate complex $[Rh(DIPAMP)(MeOH)_2]BF_4$ in the presence of added sodium halides (Cl, Br, I).[58]

When the hydrogenation catalyst [Rh(DIPAMP)(MeOH-d_4)$_2$]BF_4 and the prochiral olefin ((*Z*)-3-[1-(dimethylamino)-2-methylpent-2-en-3-yl]phenol),[62] are dissolved in methanol-d_4 in a 1 : 10 ratio, the ^{31}P NMR spectrum shows that almost 34 % of the total signal intensity corresponds to the catalytically inactive trinuclear μ_3-chloro-bridged complex $[Rh_3(DIPAMP)_3(\mu_3\text{-}Cl)_2]BF_4$, resulting from traces of chloride left in the substrate after its synthesis, Figure 14.

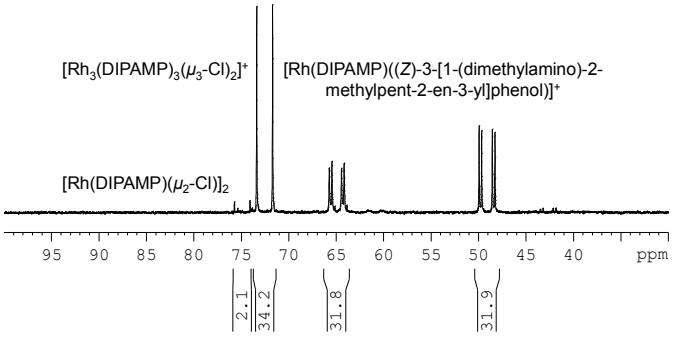

Figure 14 $^{31}P\{^1H\}$-NMR spectrum of a solution of $[Rh(DIPAMP)(MeOH\text{-}d_4)_2]BF_4$ and (3-[(2*R*,3*S*)-1-(dimethylamino)-2-methylpentan-3-yl]phenol in a 1 : 10 molar

ratio. 34 % of the signal intensity correspond to the doublet of the trinuclear complex $[Rh_3(DIPAMP)_3(\mu_3\text{-}Cl)_2]BF_4$.

Like in the competitive inhibition in enzymatic catalysis, halides compete with the substrate for the solvent complex: the amount of trinuclear complex and thus the decrease in activity they cause depends on the relative concentrations of halides and substrate and on the stability constants of the complexes they form with the metal. To prevent deactivation, special care should be paid to substrate purification, especially on industrial scale where very high substrate to catalyst ratios are used.

To summarize, from cationic rhodium complexes, often employed as catalyst, di- and trinuclear complexes may be formed: the nature of these species is affected by the diphosphine ligand (whether it contains aromatic moieties or not), the solvent (whether coordinating or not) the presence of additives (pH of the solution). These polynuclear species are not active in catalysis and need to be converted, when possible, into active species.

5. Catalyst deactivation due to irreversible reactions of the active catalyst

The rate of itaconic acid hydrogenation with the rhodium-DIPAMP catalyst in methanol decreases with increasing substrate concentration.[63] Inhibition by the substrate had already been described in 1979.[64] The X-ray structure of single crystals isolated from a solution of $[Rh(DIPAMP)(MeOH)_2]BF_4$ and itaconic acid revealed an unexpected tridentate coordination[65] of the 'hydrogenated' product to the catalyst involving the two carboxylate oxygens and oxidative addition of the C(2)-H bond to the Rh(I) centre Figure 15 left. This is in contrast to the most frequently observed substrate coordination mode which involves chelation to the metal through the C-C double bond and one carboxylate oxygen.[66]

The isolated Rh(III)-alkyl complex represents a dead-end in hydrogenation because oxidative addition of molecular hydrogen is formally impossible on a Rh(III) complex. By systematic investigation into the influence of different parameters on the formation of this complex, namely substrate concentration, reaction time, temperature, acidic and basic additives, it could be shown that its formation indeed explains the inhibiting effect of increasing substrate concentration.

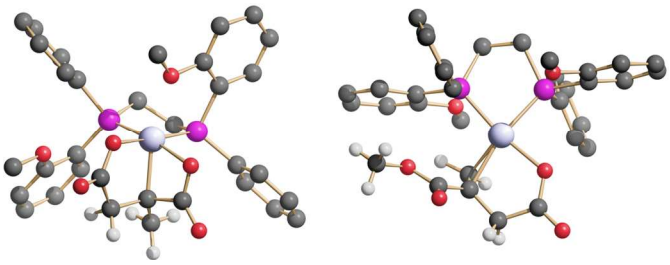

Figure 15 X-ray structures of [Rh((*S,S*)-DIPAMP)(2-methyl succinate)] (left) and [Rh((*S,S*)-DIPAMP)(α-monomethyl itaconate)] (right). Hydrogen atoms on the ligand DIPAMP are omitted for clarity.

Figure 16 illustrates the proposed mechanism for the formation of the Rh(III) alkyl complex. In the first step, the *β*-carboxylic group in the diastereomeric substrate complexes is deprotonated and coordinates to the metal as carboxylate. Figure 15 right shows the X-ray structure of the α-monomethyl ester analogue.

The *α*-carboxylic group then oxidatively adds to rhodium generating a Rh(III) hydride species. The double bond then quickly inserts into the Rh-H bond at room temperature generating the Rh(III)-alkyl complex. The rate of hydrogenation, that is the turnover frequency of the hydrogenation cycle, can be increased by raising the hydrogen pressure. The parallel and irreversible formation of the inactive Rh(III)-alkyl complex is favoured by a higher concentration of the substrate, that is of the substrate rhodium complex. At lower substrate concentrations, however, the overall reaction time is shorter, and deactivation is less obvious.

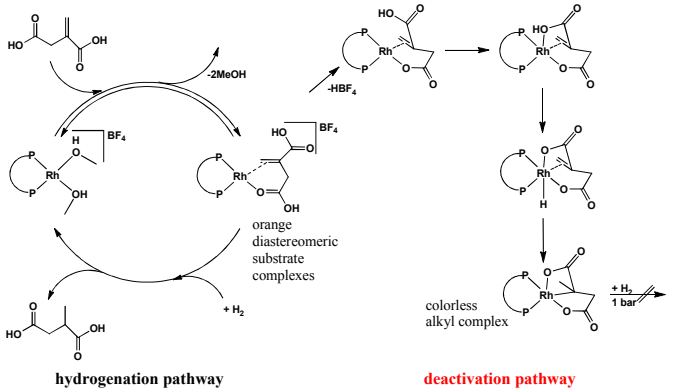

Figure 16 Catalytic cycle for itaconic acid hydrogenation (hydrogenation pathway) and catalyst deactivation pathway leading to inactive Rh(III)-alkyl complexes.

6. 'in situ' generation of precatalysts

Neutral μ_2-bridged dinuclear rhodium complexes of the type $[Rh(diphosphine)(\mu_2\text{-}X)]_2$ (X = Cl or, more rarely OH), (Figure 17, left, shows the X-ray structure of $[Rh(Xantphos)(\mu_2\text{-}Cl)]_2$) are applied as catalysts in several processes e.g. hydrogenation of prochiral olefins,[67] ketones,[68] CO_2[69] and polynuclear heteroaromatic compounds,[70] ring opening of oxa- and azabicyclic alkenes,[71] hydrogen mediated C-C bond formation,[72] addition of carboxylic acids to alkynes,[73] CO gas free hydroformylation and[74] carbonylations,[75] Pauson-Khand-type reactions,[76] olefin isomerisation,[77] cycloadditions,[78] coupling of aldehydes and allenes,[79] 1,4 addition of organoboronic acids.[80]

They are usually prepared *in situ* by addition of diphosphine ligands to rhodium alkene complexes like $[Rh(diolefin)(\mu_2\text{-}X)]_2$ or $[Rh(monoolefin)_2(\mu_2\text{-}Cl)]_2$ (monoolefins = cyclooctene, coe,

or ethylene, C_2H_4), and ligand exchange according to Scheme 4.

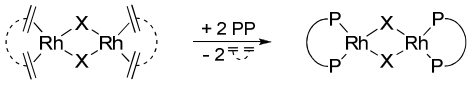

Scheme 4 Synthesis of [Rh(diphosphine)(μ_2-X)]$_2$ (X = Cl or OH) from [Rh(diolefin)(μ_2-X)]$_2$.

Systematic investigations have shown however that the *in situ* procedure affords not only the desired species but, depending on the diphosphine ligand, the rhodium precursor, the solvent and the temperature, other species are formed such as [(diolefin)Rh(μ_2-Cl)$_2$Rh(diphosphine)], Rh(diphosphine)(diolefin)]$^+$, [Rh(diphosphine)$_2$]$^+$ and [Rh(diphosphine)(diolefin)(Cl)], in other words the *in situ* procedure can be far less selective than Scheme 4 implies. In some cases, the target compound is not formed at all.[81] Figure 17, right, shows the X-ray structure of the penta coordinated rhodium complex [Rh(Xantphos)(nbd)(Cl)] (Xantphos = 4,5-Bis(diphenylphosphino)-9,9-dimethylxanthene), as the main reaction product (70 %) arising from the attempted *in situ* synthesis of [Rh(Xantphos)(μ_2-Cl)]$_2$ according to Scheme 4: as a matter of fact, the desired dimer is not formed at all.

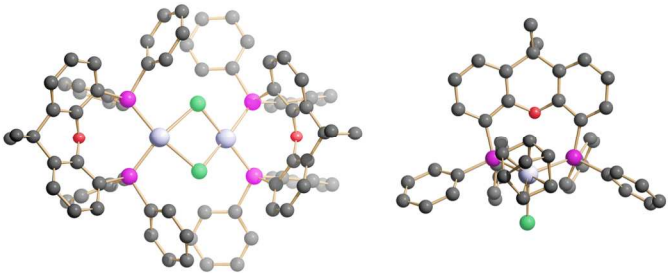

Figure 17 X-ray structures of [Rh(Xantphos)(μ_2-Cl)]$_2$ (left) and [Rh(Xantphos)(nbd)(Cl)] (right). Hydrogen atoms are omitted for clarity.[82]

The *in situ* formation of the dinuclear rhodium complex [Rh(BINAP)(μ_2-Cl)]$_2$ from the *cod* precursor [Rh(cod)(μ_2-Cl)]$_2$ and two equivalents of BINAP in either tetrahydrofuran or toluene is practically quantitative.[80,83] If the *nbd*-precursor is used instead only 80 % of the target compound is obtained in tetrahydrofuran, as the top ^{31}P spectrum in Figure 18, shows, the rest being [Rh(BINAP)(nbd)(Cl)]. In dichloromethane, selectivity drops to 22 % and most of the rhodium is engaged in the pentacoordinated species [Rh(BINAP)(nbd)(Cl)] (Figure 18, middle spectrum). In methanol, the cationic complex [Rh(BINAP)(nbd)]$^+$ is the only detectable species, Figure 18, bottom spectrum (the chloride obviously acts as counteranion and is not covalently bound to the metal).[81]

A further example of the dramatic effect of the nature of the olefin rhodium precursor on the outcome of the *in situ* procedure is provided by the case of the ligand DIOP (DIOP = 4,5-bis(diphenylphosphinomethyl)-2,2-dimethyl-1,3-dioxolane). When the cod precursor is used, only 36 % of the applied rhodium ends up in the desired [Rh(DIOP)(μ_2-Cl)]$_2$, the rest is distributed among several species so far unidentified (Figure 19, top ^{31}P spectrum).

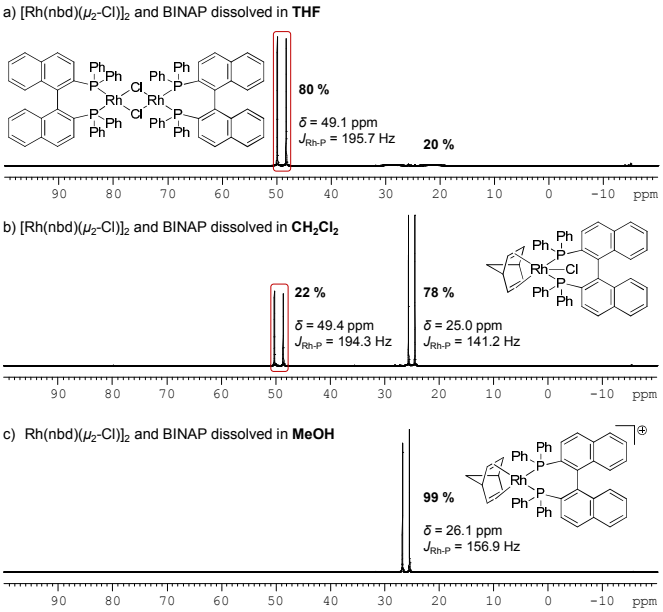

Figure 18 ^{31}P-NMR spectra of the reaction solution of the *in situ* ligand exchange between [Rh(nbd)(μ_2-Cl)]$_2$ and BINAP (1 : 2) at room temperature in top a) tetrahydrofurane, middle b) dichloromethane and bottom c) methanol.

With the nbd precursor just 0.5 % is in the form of [Rh(DIOP)(μ_2-Cl)]$_2$, the main species is actually unknown (Figure 19, middle spectrum). The best precursor is then [Rh(coe)(μ_2-Cl)]$_2$ from which 74 % of [Rh(DIOP)(μ_2-Cl)]$_2$ can be obtained. (Figure 19, bottom spectrum)[81] This can be purified only by crystallization.

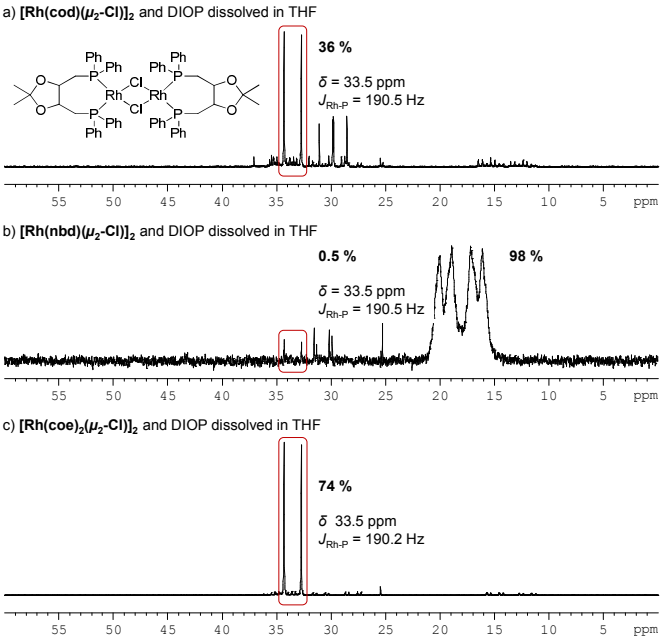

Figure 19 ^{31}P-NMR spectra of the reaction solution of the *in situ* ligand exchange of a) [Rh(*cod*)(μ_2-Cl)]$_2$, b) [Rh(*nbd*)(μ_2-Cl)]$_2$ and c) [Rh(*coe*)$_2$(μ_2-Cl)]$_2$ with DIOP (1 : 2) in tetrahydrofuran at room temperature.

The above examples concerning BINAP and DIOP clearly show that also the kind of diphosphine may steer the course of the *in situ* synthesis. Another critical factor is temperature. The *in situ* formation of $[Rh(DPPE)(\mu_2\text{-}Cl)]_2$ from $[Rh(cod)(\mu_2\text{-}Cl)]_2$ requires elevated temperatures and was achieved at 120 °C in toluene.[49c] If the reaction is carried out in tetrahydrofuran at *room temperature* – as usual for the *in situ* procedure - a precipitate is formed (95 % yield) which could be identified as the known complex $[Rh(DPPE)_2][Rh(cod)(Cl)_2]$.[84]

With Me-DuPHOS $[Rh(Me\text{-}DuPHOS)(\mu_2\text{-}Cl)]_2$ was obtained in quantitative yield at –78 °C. At room temperature in tetrahydrofuran the *in situ* procedure resulted in the formation of 60 % $[Rh(Me\text{-}DuPHOS)(\mu_2\text{-}Cl)]_2$, 8 % of the intermediate $[(Me\text{-}DuPHOS)Rh(\mu_2\text{-}Cl)_2Rh(cod)]$ and 32 % of the cationic complex $[Rh(Me\text{-}DuPHOS)_2]^+$.[81]

These examples have shown that the frequently applied *in situ* procedure for the practical generation of the catalyst precursor $[Rh(diphosphine)(\mu_2\text{-}X)]_2$ may fail to provide the desired species in quantitative yield. Unless a systematic investigation is carried out, wrong assumptions may be drawn concerning the real nature of the catalyst. In some cases, species other than the target precatalyst are prevalent in solution whose catalytic behavior in terms of activity may be deleterious, giving rise to inactivation effects and to uneconomical use of the precious metal.

7. Conclusions

Examples have been provided of the several factors which may affect the activity of rhodium diphosphine catalysts. They come into play already in the very early stages of the process when the catalytically active species is generated from a stable catalyst precursor, before it can interact with substrate and reagents. The ensuing coordinatively unsaturated intermediates may undergo aggregation phenomena to less reactive polynuclear species. The step of catalyst generation is often overlooked, when for the sake of simplicity, an *in situ* procedure is applied, despite the fact that it may be quite unselective and afford species with diminished activity, if any. We hope that this review, although focused on rhodium diphosphine complexes, may serve as a more general guide towards catalyst activity optimization having highlighted the possible sources of catalyst inhibition: competitive binding of strongly coordinating solvents, additives, substrates and products. Here, kinetics, supported by the characterization of possible reaction intermediates by NMR spectroscopy and X-ray analysis, is especially useful as the formation of inactive species and their influence on activity is regulated by the relative concentrations of the inhibitors and the stability constants of the complexes they form with the metal.

Notes and references

[a] Leibniz-Institut für Katalyse e.V. an der Universität Rostock Albert-Einstein-Strasse 29a, 18059 Rostock (Germany)
Fax: (+49)381-1281-51183
E-mail: detlef.heller@catalysis.de
[b] Address here.

1 P. Anastas, N. Eghbali, *Chem. Soc. Rev.* **2010**, *39*, 301–312.
2 *"Catalysis without precious metals"*, ed. R. Morris Bullock, **2010** Wiley-VCH Verlag & Co. KGaA.
3 A. Cornish-Bowden, *"Fundamentals of Enzyme Kinetics"*, Wiley-Blackwell, **2012**.
4 a) P. W. N. M. van Leeuwen, J. C. Chadwick, *„Homogeneous Catalysts Activity – Stability – Deactivation"*,Wiley-VCH, **2011**. b) D. Heller, A. H. M. de Vries, J. G. de Vries, *„Catalyst Inhibition and Deactivation in Homogeneous Hydrogenation"*, chapter 44 in „Handbook of Homogeneous Hydrogenation" ed. by H. G. deVries and C. Elsevier, 1483–1516, **2007**.
5 J. A. Osborn, F. H. Jardine, J. F. Young, G. Wilkinson, *J. Chem. Soc. A* **1966**, 1711–1732.
6 R. H. Crabtree, "*The Organometallic Chemistry of Transition Metals*", John Wiley & Sons, Inc., **2005**.
7 D. Steinborn, *"Fundamentals of Organometallic Catalysis"*, Wiley-VCH, **2012**.
8 D. Heller, H.-J. Drexler, J. You, W. Baumann, K. Drauz, H.-P. Krimmer, A. Börner, *Chem. Eur. J.* **2002**, *8*, 5196–5202.
9 a) U. Nagel, E. Kinzel, J. Andrade, G. Prescher, *Chem. Ber.* **1986**, *119*, 3326–3343. b) U. Nagel, T. Krink, *Angew. Chem. Int. Ed. Engl.* **1993**, *32*, 1052–1054.
10 D. Selent. D. Heller, "*In-situ Techniques for Homogeneous Catalysis*", chapter 23 in "*Catalysis From Principle to Application*" ed's M. Beller, A. Renken, R. vanSanten, 465–492, Wiley-VCH, **2012**.
11 a) H.-J. Drexler, W. Baumann, A. Spannenberg, C. Fischer, D. Heller, *J. Organomet. Chem.* **2001**, *621*, 89–102. b) W. Baumann, S. Mansel, D. Heller, S. Borns, *Mag. Res. Chem.* **1997**, *35*, 701-706.
12 C. J. Cobley, I. C. Lennon, R. McCague, J. A. Ramsden, A. Zanotti-Gerosa, *Tetrahedron Lett.* **2001**, *42*, 7481–7483.
13 a) A. Meißner, H.-J. Drexler, S. Keller, C. Selle, V. Ratovelomanana-Vidal, D. Heller, submitted for publication b) A. Preetz, C. Fischer, C. Kohrt, H.-J. Drexler, W. Baumann, D. Heller, *Organometallics*, **2011**, *30*, 5155–5159. c) G. L. Moxham, H. E Randell-Sly, S. K. Brayshaw, R. L. Woodward, A. S. Weller, M. C. Willis, *Angew. Chem. Int. Ed.* **2006**, *45*, 7618–7622.
14 a) D. Heller, K. Kortus, R. Selke, *Liebigs Ann.* **1995**, 575–581. b) W. Braun, A. Salzer, H.-J. Drexler, A. Spannenberg, D. Heller, *Dalton Trans.* **2003**, 1606–1613. c) A. Preetz, H.-J. Drexler, C. Fischer, Z. Dai, A. Börner, W. Baumann, A. Spannenberg, R. Thede, D. Heller, *Chem. Eur. J.* **2008**, *14*, 1445–1451. d) D. Heller, S. Borns, W. Baumann, R. Selke, *Chem. Ber.* **1996**, *129*, 85–89.
15 M. Baseda Krüger, Ph. D. thesis, Universität Rostock, **2013**.
16 L. Greiner, M. B. Ternbach, *Adv. Synth. Catal.* **2004**, *346*, 1392–1396.
17 a) E. Alberico, W. Baumann, J. G. de Vries, H.-J. Drexler, S. Gladiali, D. Heller, H. J. W. Henderickx, L. Lefort, *Chem. Eur. J.* **2011**, *17*, 12683–12695. b) M. van den Berg, Ph. D. Thesis, University of Groningen (The Netherlands), **2006**; http://dissertations.ub.rug.nl/faculties/science/2006m.van.den.berg/.

c) M. A. Esteruelas, J. Herrero, M. Martin, M. L. A. Oro,V. M. Real, *J. Organomet. Chem.* **2000**, *599*, 178–184.

18 Due to isobaric conditions the determined pseudo rate constants still contain the hydrogen concentration in solution, which is proportional to the overall pressure above the solution under consideration which includes the solvent vapor pressure.

19 A. Preetz, W. Baumann, C. Fischer, H.-J. Drexler, T. Schmidt, R. Thede, D. Heller, *Organometallics* **2009**, *28*, 3673–3677.

20 Unpublished results, the ligand was kindly provided by Dr. M. Stephan. (B. Zupancic, B. Mohar, M. Stephan, *Org. Lett.* **2010**, *12*, 1296–1299.)

21 C. Fischer, R. Thede, C. Selle, W. Baumann, H.-J. Drexler, D. Heller, submitted for publication.

22 C. Fischer, S. Schulz, H.-J. Drexler, C. Selle, M. Lotz, M. Sawall, K. Neymeyr, D. Heller, *ChemCatChem* **2012**, *4*, 81–88.

23 C. Fischer, C. Kohrt, H.-J. Drexler, W. Baumann, D. Heller, *Dalton Trans.* **2011**, *40*, 4162–4166.

24 A. Preetz, H.-J. Drexler, S. Schulz, D. Heller, *Tetrahedron Asymm.* **2010**, *21*, 1226–1231.

25 J. M. Brown, P. A. Chaloner, *Tetrahedron Lett.* **1978**, *19*, 1877–1880. b) J. M. Brown, P. A. Chaloner, *J. Am. Chem. Soc.* **1980**, *102*, 3040–3048.

26 J. G. de Vries, L- Lefort *„High-Throughput Experimentation and Ligand Libraries"*, chapter 36 in „Handbook of Homogeneous Hydrogenation" ed. by H. G. de Vries and C. Elsevier, 1245–1278, **2007.**

27 V. I. Tararov, R. Kadyrov, T. H. Riermeier, A. Börner, *Adv. Synth. Catal.* **2002**, *344*, 200–208.

28 a) R. R. Shrock, J. A. Osborn, *J. Am. Chem. Soc.* **1971**, *93*, 3089–3091. b) J. M. Townsend, J. F. Blount, *Inorg. Chem.* **1981**, *20*, 269–271.

29 a) R. Benn, A. Rufińska, *Angew. Chem. Int. Ed.* **1986**, *25*, 861–881, b) W. von Philipsborn, *Chem. Soc. Rev.* **1999**, *28*, 95–105.

30 a) J. M. Ernsting, C. J. Elsevier, W. G. J. de Lange, K. Timmer, *Magn. Reson. Chem.* **1991**, *29*, S118–S124. b) W. Leitner, M. Bühl, R. Fornika, C. Six, W. Baumann, E. Dinjus, M. Kessler, C. Krüger, A. Rufińska, *Organometallics* **1999**, *18*, 1196–1206.

31 B. E. Mann, *Adv. Organomet. Chem.* **1974**, *12*, 135–213. b) G. M. Bodner, L. J. Todd, *Inorg. Chem.* **1974**, *13*, 360–363.

32 D. Heller, H.-J. Drexler, A. Spannenberg, B. Heller, J. You, W. Baumann, *Angew. Chem. Int. Ed.* **2002**, *41*, 777–780.

33 a) C. Fischer, R. Thede, H.-J. Drexler, A. König, W. Baumann, D. Heller, *Chem. Eur. J.* **2012**, *18*, 11920–11928. b) C. Fischer, A. König, H.-J. Drexler, D. Heller, *Zeitschr. Anorg. Allg. Chem.* **2012**, 638, 905–906.

34 a) T. P. Dang, H. B. Kagan, *J. Chem. Soc., Chem. Commun.* **1971**, 481. b) .E. I. Klabunowski, Y. T. Struchkov, A. A. Voloboev, A. I. Yanovsky, V. A. Pavlov, *J. Mol. Catal.* **1988**, *44*, 217–243.

35 a) B. J. Holliday, Y.-M. Jeon, C. A. Mirkin, C. L. Stern, C. D. Incarvito, L. N. Zakharov, R. D. Sommer, A. L. Rheingold, *Organometallics* **2002**, *21,* 5713–5725. Resp. with 'monodentade' phosphine lignads: b) A. Meissner, C. Selle, H.-J. Drexler D. Heller, *Acta Cryst.* **2012**, *E68*, m259. c) P. Marcazzan, B. O. Patrick, B. R. James *Organometallics* **2003**, *22,* 1177–1179.

36 M. J. Burk, C. S. Kalberg, A. Pizzano, *J. Am. Chem. Soc.* **1998**, *120*, 4345–4353.

37 G. Zhu, Z. Chen, X. Zhang, *J. Org. Chem.* **1999**, *64*, 6907–6910.

38 D. Heller, J. Holz, H.-P. Drexler, J. Lang, K. Drauz, H.-P. Krimmer, A. Börner, *J. Org. Chem.* **2001**, *66*, 6816–6817.

39 A. S. C. Chan, J. J. Pluth, J. Halpern, *Inorg. Chim. Acta* **1979**, *37*, L477–L479.

40 J. Halpern, D. P. Riley, A. S. C. Chan, J. S. Pluth, *J. Am. Chem. Soc.* **1977**, *99*, 8055–8057.

41 a) R. Kuwano, M. Kashiwabara, K. Saito, T. Ito, K. Kaneda, Y. Ito, *Tetrahedron Asymmetry* **2006**, *17*, 521–535. b) K. Junge, G. Oehme, A. Monsees, T. Riermeier, U. Dingerdissen, M. Beller, *J. Organomet. Chem.* **2003**, *675*, 91–96. c) J. Holz, A. Kless, S. Borns, S. Trinkhaus, R. Selke, D. Heller, *Tetrahedron: Asymmetry* **1995**, *6*, 1973–1988. d) M. J. Burk, M. F. Gross, J. P. Martinez, *J. Am. Chem. Soc.* **1995**, *117*, 9375–9376.

42 a) Halpern, A. S. C. Chan, D. P. Riley, J. J. Pluth, *Adv. Chem. Ser.* **1979**, *173*, 16–25. b) C. R. Landis, J. Halpern, *Organometallics* **1983**, *2*, 840–842. c) M. J. Burk, F. Bienewald, S. Challenger, A. Derrick, J. A. Ramsden, *J. Org. Chem.* **1999**, *64*, 3290–3298.

43 I. D. Gridnev, N. Higashi, K. Asakura, T. Imamoto, *J. Am. Chem. Soc.* **2000**, *122*, 7183–7194.

44 I. D. Gridnev, M. Yasutake, N. Higashi, T. Imamoto, *J. Am. Chem. Soc.* **2001**, *123*, 5268–5276.

45 a) P. Hübler, J. Bargon, *Angew. Chem. Int. Ed.* **2000**, *39*, 3701–3703. b) P. Hübler, R. Giernoth, G. Kümmerle, J. Bargon, *J. Am. Chem. Soc.* **1999**, *121*, 5311–5318. c) R. Giernoth, P. Hübler, J. Bargon, *Angew. Chem., Int. Ed. Engl.* **1998**, *37*, 2473–2475.

46 R. H. Crabtree, M. F. Mellea, J. M. Quirk, *J. Chem. Soc., Chem. Comm.* **1981**, 1217–1218.

47 Connors, K. A.; "*Binding Constants – The Measurement of Molecular Complex Stability"* John Wiley & Sons: Madison-Wisconsin, **1987**, Chapter 4.

48 M. Schwarze, J.-S. Milano-Brusco, V. Strempel, T. Hamerla, S. Wille, C. Fischer, W. Baumann, W. Arlt, R. Schomäcker, *RSC adv.* **2011**, *1*, 474–483.

49 a) R. W. Barnhart, X. Wang, P. Noheda, S. H. Bergens, J. Whelan, B. Bosnich, *Tetrahedron* **1994**, *50*, 4335–4346. b) D. P. Fairlie, B. Bosnich, *Organometallics* **1988**, *7*, 946–954 c) D. P. Fairlie, B. Bosnich, *Organometallics* **1988**, *7*, 936–945.

50 a) K. Mikami, S. Kataoka, Y. Yusa, K. Aikawa, *Org. Lett.* **2004**, *6*, 3699–3701. b) K. Mikami, Y. Yusa, M. Hatano, K. Wakabayashi, K. Aikawa, *Chem. Commun.* **2004**, 98–99. c) R. W. Barnhart, X. Wang, P. Noheda, S. H. Bergens, J. Whelan, B. Bosnich, *Tetrahedron* **1994**, *50*, 4335–4346. d) D. G. Allen, S. B. Wild, D. L. Wood, *Organometallics* **1986**, *5*, 1009–1015. e) A. Miyashita, H. Takaya, T. Souchi, R. Noyori, *Tetrahedron* **1984**, *40*, 1245–1253. f) D. P. Riley, *J. Organomet. Chem.* **1982**, *234*, 85–97. g) A. Miyashita, A. Yasuda, H. Takaya, K. Toriumi, T. Ito, T. Souchi, R. Noyori, *J. Am. Chem. Soc.* **1980**, *102*, 7932–7934.

51 a) I. D. Gridnev, E. Alberico, S. Gladiali *Chem. Commun*. **2012**, *48*, 2186–2188. b) I. D. Gridnev, C. Fan, P. G. Pringle, *Chem. Commun.* **2007**, 1319–1321. c) A. Rifat, N. J. Patmore, M. F. Mahon, A. S. Weller, *Organometallics* **2002**, *21*, 2856–2865. d) P. Marcazzan, M.

B. Ezhova, B. O. Patrick, B. R. James, *C. R. Chim.* **2002**, *5*, 373–378. e) For redox-switchable ligand see, for example: E. T. Singewald, C. A. Mirkin, C. L. Stern, *Angew. Chem. Int. Ed.* **1995**, *35*, 1624–1627.

52 Hydrogen-mediated reductive C-C coupling: a)Y. Lu, S. K. Woo, M. J. Krische, *J. Am. Chem. Soc.* **2011**, *133*, 13876–13879. b) J. R. Kong, M. J. Krische, *J. Am. Chem. Soc.* **2006**, *128*, 16040–16041. c) J.-R. Kong, C.-W. Cho, M. J. Krische, *J. Am. Chem. Soc.* **2005**, *127*, 11269–11276.
Enantioselective reductive cyclization: d) J. U. Rhee, M. J. Krische, *J. Am. Chem. Soc.* **2006**, *128*, 10674–10675. e) H.-Y. Jang, F. W. Hughes, H. Gong, J. Zhang, J. S. Brodbelt, M. J. Krische, *J. Am. Chem. Soc.* **2005**, *127*, 6174–6175.
Intermolecular cyclotrimerization: f) K. Masutomi, N. Sakiyama, K. Noguchi, K. Tanaka, *Angew. Chem. Int. Ed.* **2012**, *51*, 13031–13035. g) N. Sakiyama, K. Noguchi, K. Tanaka, *Angew. Chem. Int. Ed.* **2012**, *51*, 5976–5980. h) M. Ishida, Y. Shibata, K. Noguchi, K. Tanaka, *Chem. Eur. J.* **2011**, *17*, 12578–12581. i) Y. Miyauchi, M. Kobayashi, K. Tanaka, *Angew. Chem. Int. Ed.* **2011**, *50*, 10922–10926. and references cited therein.

53 Reference [50b]: "…the cationic Rh(I)(PP-ligand) dimer complexes are usually unstable to isolation or are difficult to store in solution for any length of time even at low temperature,…"

54 H.-Y. Jang, M. J. Krische, *J. Am. Chem. Soc.* **2004**, *126*, 7875–7880.

55 A. Preetz, H.-J. Drexler, D. Heller, unpublished results.

56 T. Yamagata, K. Tani, Y. Tatsuno, T. Saito, *J. Chem. Soc., Chem. Comm.* **1988**, 466–468.

57 A. Preetz, W. Baumann, H.-J. Drexler, C. Fischer, J. Sun, A. Spannenberg, O. Zimmer, W. Hell, D. Heller, *Chem. Asian. J.* **2008**, *3*, 1979–1982.

58 A. Preetz, C. Kohrt, A. Meißner, S. Wei, H.-J. Drexler, H. Buschmann, D. Heller, *Catal. Sci. Technol.* **2013**, *3*, 462–468.

59 Although the formation of trinuclear rhodium complexes had already been described by Saito,[54] their reversible formation has been experimentaly proven through the reaction of the intermediate $[Rh_2(Me\text{-}DuPHOS)_2(\mu_2\text{-}Cl)_2]$ with the cationic complex $[Rh(Me\text{-}DuPHOS)(THF)_2]BF_4$].[58]

60 [2-(3-Methoxy-phenyl)-cyclohex-1-enylmethyl]-dimethylamine is a member of a class of 1,2-disubstituted cyclohexene derivatives which are important intermediates in the synthesis of pharmaceutical active compounds acting on the central nervous system and can be transformed by a stereoselective hydrogenation to *Tramadol*, an important world-wide used analgesic drug.

61 C. J. Cobley, I. C. Lennon, C. Praquin, A. Zanotti-Gerosa, *Org. Proc. Res. & Dev.* **2003**, *7*, 407–411.

62 The prochiral olefin (*Z*)-3-[1-(Dimethylamino)-2-methylpent-2-en-3-yl]phenol is also an important precursor of the new analgesic drug *Tapentadol* which is as an open-chain analogue of *Tramadol*. The (*R*,*R*) stereoisomer of *Tapentadol* is a novel, centrally acting analgesic with a dual mode of action: μ-opioid receptor (MOR) agonism and norepinephrine reuptake inhibition.

63 a) T. Schmidt, H.-J. Drexler, J. Sun, Z. Dai, W. Baumann, A. Preetz, D. Heller, *Adv. Synth. Catal.* **2009**, *351*, 750–754. b) T. Schmidt, W. Baumann, H.-J. Drexler, D. Heller, *J. Organomet. Chem.* **2011**, *696*, 1760–1767.

64 W. C. Christopfel, B. D. Vineyard, *J. Am. Chem. Soc.* **1979**, *101*, 4406–4408.

65 J. M. Brown, D. Parker, *J. Org. Chem.* **1982**, *47*, 2722–2730.

66 T. Schmidt, Z. Dai, H.-J. Drexler, W. Baumann, C. Jäger, D. Pfeifer, D. Heller, *Chem. Eur. J.* **2008**, *14*, 4469–4471.

67 a) Y. Hsiao, N. R. Rivera, T. Rosner, S. W. Krska, E. Njolito, F. Wang, Y. K. Sun, J. D. Armstrong III, E. J. J. Grabowski, R. D. Tillyer, F. Spindler, C. Malan, *J. Am. Chem. Soc.* **2004**, *126*, 9918–9919. b) H. B. Kagan, T. P. Dang, *J. Am. Chem. Soc.* **1972**, *94*, 6429–6433.
Industrial applications: c) C. S. Shultz, S. W. Krska, *Acc. Chem. Res.* **2007**, *40*, 1320–1326. d) G. Beck, *Synlett* **2002**, *6*, 837–850. e) H. Jendralla, B. Seuring, J. Herchen, B. Kulitzscher, J. Wunner, W. Stüber, R. Koschinsky, *Tetrahedron* **1995**, *51*, 12047–12068.

68 a) J.-F. Carpentier, A. Mortreux, Tetrahedron: *Asymmetry* **1997**, *8*, 1083–1099. b) A. Roucoux, L. Thieffry, J.-F. Carpentier, M. Devocelle, C. Meliet, F. Agbossou, A. Mortreux, *Organometallics* **1996**, *15*, 2440–2449.

69 W. Leitner, E. Dinjus, F. Gaßner, *J. Organomet. Chem.* **1994**, *475*, 257–266.

70 T. J. Kim, K. C. Lee, *Bull. Korean Chem. Soc.* **1989**, *10*, 279–282.

71 a) G. C. Tsui, M. Lautens, *Angew. Chem.* **2012**, *124*, 5496–5500. *Angew. Chem. Int. Ed.* **2012**, *51*, 5400–5404. b) A. Preetz, C. Kohrt, H.-J. Drexler, A. Torrens, H. Buschmann, M. G. Lopez, D. Heller, *Adv. Synth. Catal.* **2010**, *352*, 2073–2080. c) K. Fagnou, in: *Modern Rhodium-Catalyzed Organic Reactions*, (Ed. P. A. Evans), Wiley-VCH, Weinheim, **2005**, chapter 9, 173–190. d) M. Lautens, K. Fagnou, *Proc. Natl. Acad. Sci. USA* **2004**, *101*, 5455–5460.

72 a) C.-W. Cho, M. J. Krische in *Handbook of Homogeneous Hydrogenation* (Hrsg.: J. G. de Vries, C. J. Elsevier), WILEY-VCH, Weinheim, **2007**, ch. 22, 713–741. c) H.-Y. Jang, M. J. Krische, *Acc. Chem. Res.* **2004**, *37*, 653–661.

73 a) A. Lumbroso, N. R. Vautravers, B. Breit, *Org. Lett.* **2010**, *12*, 5498–5501. b) A. Lumbroso, P. Koschker, N. R. Vautravers, B. Breit, *J. Am. Chem. Soc.* **2011**, *133*, 2386–2389.

74 G. Makado, T. Morimoto, Y. Sugimoto, K. Tsutsumi, N. Kagawa, K. Kakiuchi, *Adv. Synth. Catal.* **2010**, *352*, 299–304.

75 a) T. Morimoto, M. Fujioka, K. Fuji, K. Tsutsumi, K. Kakiuchi, *J. Organomet. Chem.* **2007**, *692*, 625–634. b) K. Fuji, T. Morimoto, K. Tsutsumi, K. Kakiuchi, *Chem. Commun.* **2005**, 3295–3297.

76 a) K. Fuji, T. Morimoto, K. Tsutsumi, K. Kakiuchi, *Tetrahedron Letters* **2004**, *45*, 9163–9166. b) K. Fuji, T. Morimoto, K. Tsutsumi, K. Kakiuchi, *Angew. Chem. Int. Ed.* **2003**, *42*, 2409–2411.

77 D. M. Ohlmann, L. J. Gooßen, M. Dierker, *Chem. Eur. J.* **2011**, *17*, 9508–9519.

78 F. Inagaki, K. Sugikubo, Y. Oura, C. Mukai, *Chem. Eur. J.* **2011**, *17*, 9062–9065.

79 T. Toyoshima, T. Miura, M. Murakami, *Angew. Chem. Int. Ed.* **2011**, *50*, 10436–10439.

80 T. Hayashi, M. Takahashi, Y. Takaya, M. Ogasawara, *J. Am. Chem. Soc.* **2002**, *124*, 5052–5058.

81 A. Meißner, A. Preetz, H.-J. Drexler, W. Baumann, A. Spannenberg, A. König, D. Heller, submitted for publication.

82 Diffraction data were collected at low temperature on a Bruker Kappa APEX II Duo. The structures were solved by direct methods (SHELXS-97) (G. M. Sheldrick, *Acta Cryst. A* **1997**, *64*, 112–122.) and refined by full matrix least square techniques against F^2 (SHELXL-97). XP (Siemens Analytical X-ray Instruments, Inc.) was used for structure representations. Atoms other than hydrogens were refined anisotropically. Hydrogen atoms were placed into theoretical positions and were refined by using the riding model. Contributions of solvent molecules were removed in [Rh(Xantphos)(μ_2-Cl)]$_2$ from the diffraction data with PLATON / SQUEEZE (T. Spek, *Acta Cryst. D* **2009**, *65*, 148–155.).

Crystal data for [Rh(Xantphos)(μ_2-Cl)]$_2$: $C_{78}H_{64}Cl_2O_2P_4Rh_2$, monoclinic space group *C*2/m, a = 29.9133(15), b = 18.7802(9), c = 19.2461(10) Å, β = 114.861(1)°, V = 9810.1(9) Å^3, T = 150(2) K, Z = 4, ρcalcd = 0.971 g cm^{-3}, μ(Mo Kα) = 0.488 mm^{-1}. 81146 total data, Θ_{max} = 26.00. R = 0.0307 for 8138 data with $I > 2\sigma(I)$ of 9960 unique data and 412 refined parameters. The final R_1 values were 0.0417 (all data). The final $wR(F^2)$ values were 0.0735 (all data). The goodness of fit on F^2 was 1.017.

Crystal data for [Rh(Xantphos)(nbd)Cl] * THF: $C_{50}H_{74}ClO_2P_2Rh$, triclinic space group *P*-1, a = 10.1367(13), b = 10.1518(13), c = 21.075(3) Å, α = 93.865(5), β = 102.017(5), γ = 108.917(5), V = 1985.2(4) Å^3, T = 150(2) K, Z = 2, ρcalcd = 1.472 g cm^{-3}, μ(Cu Kα) = 5.182 mm^{-1}. 28612 total data, Θ_{max} = 63.69. R = 0.0285 for 6327 data with $I > 2\sigma(I)$ of 6482 unique data and 508 refined parameters. The final R_1 values were 0.0291 (all data). The final $wR(F^2)$ values were 0.0704 (all data). The goodness of fit on F^2 was 1.098.

Crystallographic datas (excluding structure factors) for the structures reported in this paper have been deposited at the Cambridge Crystallographic Data Centre as supplementary publication no. CCDC-996813 for [Rh(Xantphos)(μ_2-Cl)]$_2$ and CCDC-996814 for [Rh(Xantphos)(nbd)Cl].Copies of the data can be obtained free of charge on application to CCDC, 12 Union Road, Cambridge, CB21EZ, UK (fax: int. code + (1223) 336-033; e-mail: deposit@ccdc.cam.ac.uk.

83 K. A. Bunten, D. H. Farrar, A. J. Poë, A. Lough, *Organometallics* **2002**, *21,* 3344–3350.

84 S. I. Lee, S. Y. Park, J. H. Park, Y. K. Chung, J. W. Han, *Bulletin of the Korean Chemical Society* **2007**, *28*, 1919–1920.

